Chem. Mater. **1996,** *8,* 721−726

Synthesis and Characterization of Novel One-Dimensional Phases from Supercritical Ammonia: $Cs_3Ag_2Sb_3S_8$, α- and *β*-Cs_2AgSbS_4, and Cs_2AgAsS_4

Paul T. Wood, George L. Schimek, and Joseph W. Kolis*

Department of Chemistry, Clemson University, Clemson, South Carolina 29634-1905

Received August 18, 1995. Revised Manuscript Received December 11, 1995[⊗]

Synthetic efforts utilizing Cs_2CO_3, Ag, M_2S_3 (M = As, Sb), and S_8 in supercritical ammonia (160 °C) have yielded four novel, one-dimensional compounds in the Cs−Ag−M−S system. These members were characterized by single-crystal X-ray diffraction and diffuse reflectance measurements. $Cs_3Ag_2Sb_3S_8$ (**I**) crystallizes in the monoclinic space group $P2_1/m$ with lattice parameters of $a = 10.539(3)$ Å, $b = 7.234\ (3)$ Å, $c = 12.777\ (3)$ Å, $\beta = 101.96\ (2)°$, $V = 952.7(9)$ Å^3, $z = 2$, and $R = 0.0377$ ($wR = 0.0445$). The columnar framework of this compound consists of $[SbS_2]_\infty{}^-$ chains and $SbS_4{}^{3-}$ tetrahedra that are stitched together by Ag(I) ions. When the Cs/Sb ratio is doubled, α- and *β*-Cs_2AgSbS_4 (**II** and **III**, respectively) are obtained. Both phases contain identical anionic chains which pack in different ways. Compound **II** crystallizes in the monoclinic space group $P2_1/c$ with $a = 6.848(3)$ Å, $b = 11.413(3)$ Å, $c = 13.187(3)$ Å, $\beta = 102.45(3)°$, $V = 1006.5(6)$ Å^{3,} $z = 4,$ and $R = 0.0414$ ($wR = 0.0498$). Compound **III** was refined in the triclinic space group $P\bar{1}$ with $a = 6.917(2)$ Å, $b = 7.341(2)$ Å, $c = 10.998(2)$ Å, $\alpha = 73.83(2)°$, $\beta = 76.08(2)°$, $\gamma = 71.71(2)°$, $V = 502.0(2)$ Å^3, $z = 2$, and $R = 0.0343$ ($wR = 0.0423$). Compound **IV**, the isostructural arsenic analog of **III**, Cs_2AgAsS_4, has also been prepared and structured: $a = 6.783(2)$ Å, $b = 7.191(2)$ Å, $c = 11.088(2)$ Å, $\alpha = 73.61(3)°$, $\beta = 75.10(3)°$, $\gamma = 70.83(3)°$, $V = 481.9(2)$ Å^3, $z = 2$, and $R = 0.0397$ ($wR = 0.0601$). The infinite, one-dimensional anionic chains in the Cs_2AgMS_4 phases are built from isolated $MS_4{}^{3-}$ tetrahedra (M = As, Sb) joined by Ag(I) ions. In all four materials the silver atoms are tetrahedrally coordinated by sulfur atoms, and cesium(I) cations are located in the surrounding voids. Bond valence sums support the electron precise counts predicted for all three members: $Cs_3{}^{I}Ag_2{}^{I}Sb_2{}^{III}Sb^{V}S_8{}^{-II}$ and $Cs_2{}^{I}Ag^{I}M^{V}S_4{}^{-II}$. Optical bandgaps determined via diffuse reflectance measurements indicate that these are wide bandgap materials (2.1−2.7eV) and thus are in agreement with the expected electronic configurations.

Introduction

The use of supercritical or superheated fluids to prepare solids[1] has opened avenues to a wide variety of novel materials.[2] These fluids can act as the solvent to solubilize reagents and thus provide a medium for better transport and/or intermixing of the reagents. The conditions necessary for supercriticality of a solvent provide a relatively high-pressure and low-temperature environment, as compared to typical solid-state synthetic conditions. These properties favor the formation of kinetically stable materials; and to a large extent, good-quality single crystals can also be obtained for analysis.

It is known that alkali-metal carbonates will induce disproportionation of elemental sulfur to polysulfides and sulfates at intermediate temperatures.[3] This provides a convenient source of group 1 polysulfides that are much easier to handle than their respective elemental forms, especially the heavier analogues. The resultant polysulfide solutions react readily with soft group 11 metals. Exploitation of this property, in the presence of a relatively large metal cation, such as that found in cesium carbonate, has been shown to promote the formation of low-dimensional materials in this laboratory.[4] Here we report the synthesis, structure, and optical bandgaps of four novel one-dimensional compounds: $Cs_3Ag_2Sb_3S_8$, α- and *β*-Cs_2AgSbS_4, and Cs_2AgAsS_4.

Experimental Procedure

The methods used to prepare the title phases rely on modifications of techniques first reported by Rabenau.[1] The starting reagents, cesium carbonate (Aldrich, 99.9%), Ag (Strem, 99.9%), Sb_2S_3 (Strem, 98%) or As_2S_3 (Johnson-Matthey, 99.9%), and S_8 (Mallinckrodt, 99.9%) were loaded into fused silica tubes (5 mm i.d., 7 mm o.d.) under an argon atmosphere in a drybox. $Cs_3Ag_2Sb_3S_8$ (**I**) can be prepared on a ∼200 mg

---

[⊗] Abstract published in *Advance ACS Abstracts,* February 1, 1996.

[1] Rabenau, A. *Angew. Chem., Int. Ed. Engl.* **1985**, *24,* 1026.

[2] For example: (a) Wood, P. T.; Pennington, W. T.; Kolis, J. W. *J. Chem. Soc.; Chem. Commun.* **1993**, 235. (b) Wood, P. T.; Pennington, W. T.; Kolis, J. W. *J. Am. Chem. Soc.* **1992**, *114*, 9233. (c) Jerome, J. E.; Wood, P. T.; Pennington, W. T.; Kolis, J. W. *Inorg. Chem.* **1994**, *33*, 1733. (d) Wood, P. T.; Pennington, W. T.; Kolis, J. W. *Inorg. Chem.* **1994**, *33*, 1556. (e) Sheldrick, W. S.; Häusler, H.-J. *Z. Anorg. Allg. Chem.* **1988**, *561*, 149. (f) Sheldrick, W. S.; Braunbeck, H. G. *Z. Naturforsch.* **1989**, *44b*, 1397. (g) Haushalter, R. C. *Chem. Mater.* **1991**, *4*, 31. (h) Liao, J.-H.; Kanatzidis, M. G. *Inorg. Chem.* **1992**, *31*, 431. (i) Jacobs, H.; Schmidt, D. *Curr. Top. Mater. Sci.* **1982**, *8*, 381. (j) Raymond, C. C.; Dorhout, P. K.; Miller, S. M. *Inorg. Chem.*, **1994**, *33*, 2703. (k) Chou, J.-H.; Kanatzidis, M. G. *Inorg. Chem.* **1994**, *33*, 1001.

[3] (a) Kanatzidis, M. G. *Chem. Mater.* **1990**, *2*, 353. (b) Schneider, R. *J. Prakt. Chem. Ser. 2* **1874**, *209*, 10.

[4] (a) Wood, P. T.; Jerome, J. E.; Pennington, W. T.; Kolis, J. W. Joint Meeting of ACS Central and Great Lakes Regions, June, 1994. (b) Schimek, G. L.; Pennington, W. T.; Kolis, J. W. ACS Great Lakes Regional Meeting, June, 1995. (c) Schimek, G. L.; Kolis, J. W., unpublished results.

Table 1. Crystallographic Data for $Cs_3Ag_2Sb_3S_8$, α- and β-Cs_2AgSbS_4, and Cs_2AgAsS_4

	I	II	III	IV
formula	$Cs_3Ag_2Sb_3S_8$	α−Cs_2AgSbS_4	β−Cs_2AgSbS_4	Cs_2AgAsS_4
fw	1236.2	623.7	623.7	576.9
color/habit	red parallelepipeds	yellow polyhedra	yellow rods	yellow plates
size, mm	0.04 × 0.05 × 0.07	0.08 × 0.08 × 0.1	0.02 × 0.03 × 0.05	0.1 × 0.1 × 0.2
cryst syst	monoclinic	monoclinic	triclinic	triclinic
space group	$P2_1/m$ (No. 11)	$P2_1/c$ (No. 14)	$P\bar{1}$ (No. 2)	$P\bar{1}$ (No. 2)
a, Å	10.539(3)	6.848(3)	6.917(2)	6.783(2)
b, Å	7.234(3)	11.413(3)	7.341(2)	7.191(2)
c, Å	12.777(3)	13.187(3)	10.998(2)	11.088(2)
α, deg	90	90	73.83(2)	73.61(3)
β, deg	101.96(2)	102.45(3)	76.08(2)	75.10(3)
γ, deg	90	90	71.71(2)	70.83(3)
V, Å^3	952.7(9)	1006.5(6)	502.0(2)	481.9(2)
Z	2	4	2	2
Dcalc, g cm^{-3}	4.309	4.115	4.126	3.975
μ, mm^{-1} (Mo Kα)	12.717	12.498	12.536	13.723
trans coeff	0.665−1.000	0.813−1.294	0.928−1.067	0.461−1.000
coll. speed, deg/min	2−15	8	8	3
2θ range, deg/octant	3.5−45/$hk\pm l$	3−50/$hk\pm l$	4−50/$\pm hk\pm l$	3.5−45/$\pm hk\pm l$
no. of data	1452	2041	1941	1381
no. of unique data	1365	1876	1764	1260
R_{int}, %	3.33	2.54	2.70	2.45
no. of data ($I > 3\sigma(I)$)	873	1153	1017	1139
no. of variables	88	73	73	73
max shift (Δ/σ)	0.001	0.001	0.001	0.002
max/min e$^-$ ρ	1.48/−1.47	1.12/−1.56	0.90/−1.33	1.22/−1.60
S	1.01	2.10	1.05	1.82
$R(F_o)$	0.0377	0.0414	0.0343	0.0397
$wR(F_o)$	0.0445	0.0498	0.0423	0.0601

scale from a stoichiometric ratio (24:32:24:7) of Cs_2CO_3, Ag, Sb_2S_3, and S_8. Likewise, Cs_2AgMS_4 (M = Sb in **II** and **III**, As in **IV**) were prepared from stoichiometric ratios (16:16:8:5) of Cs_2CO_3, Ag, M_2S_3, and S_8. The loaded tubes were subsequently evacuated (~10^{-3} Torr) and approximately 0.5 mL (~40% fill) of NH_3 was distilled onto the reagents. The tubes were sealed off after freezing the solvent and then thawed to give dark purple (**I**), bright violet (**II** and **III**), or red/brown (**IV**) solutions and some insoluble reagents. The tubes were loaded into a high-pressure autoclave and counter-pressured to 3200 psi with argon to ensure the integrity of the quartz tubes. The autoclave was heated at 160 °C for 3 days for **I**−**III** and 135 °C for 6 days for **IV**. After cooling, the liquid NH_3 was colorless and $Cs_3Ag_2Sb_3S_8$ (**I**) was observed as red parallelepipeds (65% isolated yield) with S_8 and Cs_2CO_3 remaining. Cs_2AgSbS_4 (**II** and **III**) and Cs_2AgAsS_4 (**IV**) were found as yellow polyhedra, rods, and plates, respectively, in light green NH_3 solutions. Both forms of Cs_2AgSbS_4 were isolated from the same reaction tube (26% isolated yield) and were always contaminated by $Cs_3Ag_2Sb_3S_8$ (53% yield) and S_8 and Cs_2CO_3 (21% unreacted). Cs_2AgAsS_4 can be prepared in approximately 47% isolated yield, with an unidentifiable powder, and a few crystals of a ternary phase whose structure has not been resolved, accounting for the remaining material.[4c]

Optical diffuse reflectance measurements on **I**−**IV** were made at room temperature from 200 to 800 nm with a Shimadzu UV3100 spectrophotometer equipped with an integrating sphere attachment. Barium sulfate was used as the reflectance standard. The reflectance data was converted to absorption data using the Kubelka−Munk function.[5] The optical bandgaps for Sb_2S_3 and As_2S_3 were also determined from data collected in a similar fashion and gave values within experimental error of reported values.

Crystallography. Single crystals of all four phases were mounted in capillaries with quick-drying epoxy and studied with one of the following four-circle diffractometers equipped with graphite-monochromated Mo Kα radiation (λ = 0.710 73 Å): a Nicolet R3mV (**I**), a Rigaku AFC7R (**II** and **III**), or a refurbished (Crystal Logic, Inc.) Syntex $P2_1$ (**IV**). An ω−2θ scan mode for the room-temperature (22 °C) data collections was utilized in all cases. On the basis of three standard reflections measured every 97 reflections, decay was determined to be less than ±2% for **I**−**IV**. All the intensity data were corrected for Lorentz and polarization effects. A semiempirical absorption correction (ψ-scans) was applied to the data for **I** and **IV** and a DIFABS[6] absorption correction was utilized for **II** and **III**.

The space group for **I** was chosen as $P2_1/m$, based upon the systematic absence: $0k0$, $k = 2n + 1$ and intensity data that indicated a centrosymmetric space group. Compound **II** was refined in $P2_1/c$ as determined from the systematic absences: $h0l$, $l = 2n + 1$ and $0k0$, $k = 2n + 1$. The centrosymmetric space group chosen for both **III** and **IV** was $P\bar{1}$, based on lattice parameters and statistical tests. All the structures were solved by direct methods and refined on $|F|$ by full-matrix, least-squares techniques in SHELXTL-PLUS[7] or TEXSAN.[8] All atomic thermal parameters were refined anisotropically. Crystallographic details for **I**−**IV** can be found in Table 1 and positional parameters with isotropic thermal parameters are given in Table 2.

Structural Description. Compound **I**, $Cs_3Ag_2Sb_3S_8$, consists of anionic columns separated by cesium cations. As shown in Figure 1, the $[Ag_2Sb_3S_8]^{3-}$ columns run parallel to and are centered about the b axis. Figure 2 is an ORTEP[9] representation of a piece of the infinite column as viewed perpendicular to the b axis. The building block for **I** can be generated by inversion and mirror symmetry operators. Application of the inversion operator located at the center of the Ag1−S1−Ag1a−S1a four-membered ring (the origin), followed by reflection across the mirror planes (Sb1 and S1 reside on $(x,{}^1/_4,z)$ and all cesium atoms, Sb2, Sb3, S3, S5, and S6 reside on $(x,{}^3/_4,z)$ mirror planes) generates the column which is perpetuated by unit-cell translations. The SbS_4^{3-} and $[SbS_2]_\infty^-$ groups form the outer sheath of the columns. These two group 15/16 building blocks are linked together by bridging Ag(I) ions at the core of the column. The SbS_4^{3-} groups all have two terminal vertexes with the remaining two sulfur atoms bridg-

---

(5) Wendlandt, W. W.; Hecht, H. G. *Reflectance Spectroscopy*; Interscience Publishers: New York, 1966.

(6) Walker, N.; Stuart, D. *Acta Crystallogr.* **1983**, *A39*, 158.

(7) SHELXTL-PLUS: Sheldrick, G. M. Siemens XRD, Madison, WI.

(8) TEXSAN: Single Crystal Structure Analysis Software, Version 1.6, 1993. Molecular Structure Corp., The Woodlands, TX 77381.

(9) Johnson, C. K. *ORTEP-II, A FORTRAN Thermal-Ellipsoid Plot Program*, Report ORNL-5138, Oak Ridge National Laboratory, Oak Ridge, TN, 1976.

Table 2. Atomic Coordinates ($\times 10^4$) and Equivalent Isotropic Thermal Parameters ($Å^2 \times 10^3$)[a]

	X	*Y*	*Z*	U_{eq}
		$Cs_3Ag_2Sb_3S_8$ (**I**)		
Cs1	5434(2)	2500	6608(2)	37(1)
Cs2	4194(2)	2500	0732(2)	35(1)
Cs3	8516(2)	2500	4456(2)	40(1)
Sb1	−1350(2)	7500	2128(1)	18(1)
Sb2	−1785(2)	2500	1150(1)	19(1)
Sb3	2333(2)	2500	3755(2)	18(1)
Ag1	1278(2)	5265(3)	1055(1)	41(1)
S1	−0887(7)	7500	0310(5)	24(3)
S2	−3005(5)	4981(8)	1878(4)	24(2)
S3	−3088(7)	2500	−0615(5)	21(2)
S4	1246(6)	5143(8)	2983(4)	35(2)
S5	4478(8)	2500	3598(6)	34(3)
S6	2063(9)	2500	5508(6)	32(3)
		α−Cs_2AgSbS_4 (**II**)		
Cs1	6311(2)	−2425(1)	3422(1)	43(1)
Cs2	1161(2)	−0072(1)	3346(1)	43(1)
Sb1	1955(2)	−2148(1)	0612(1)	19(1)
Ag1	2919(2)	0250(1)	−0726(1)	43(1)
S1	3844(7)	−0559(4)	1428(3)	27(2)
S2	1511(7)	−1830(4)	−1177(3)	27(3)
S3	−1164(7)	−2156(4)	1075(4)	27(2)
S4	3460(8)	−3942(4)	1047(4)	34(3)
		β-Cs_2AgSbS_4 (**III**)		
Cs1	2873(2)	2453(2)	4050(1)	37(1)
Cs2	7628(2)	−4940(2)	1923(1)	36(1)
Sb1	1307(2)	−1338(1)	2366(1)	18(1)
Ag1	3736(2)	−0875(2)	−0714(1)	39(1)
S1	2321(6)	1502(6)	1178(4)	25(2)
S2	2623(6)	−3687(6)	1110(4)	24(1)
S3	−2316(6)	−0507(6)	2744(4)	28(2)
S4	2520(7)	−2618(6)	4305(4)	31(2)
		Cs_2AgAsS_4 (**IV**)		
Cs1	2736(1)	2412(1)	4036(1)	38(1)
Cs2	7614(1)	−4898(1)	1909(1)	37(1)
As1	1397(2)	−1354(2)	2318(1)	16(1)
Ag1	3572(2)	−0789(2)	−0771(1)	36(1)
S1	2365(4)	1335(4)	1216(3)	22(1)
S2	2562(4)	−3598(4)	1149(3)	22(1)
S3	−2061(4)	−0510(4)	2756(3)	25(1)
S4	2603(5)	−2578(4)	4081(3)	27(1)

[a] Equivalent isotropic U_{eq} is defined as one-third of the trace of the orthogonalized U_{ij} tensor.

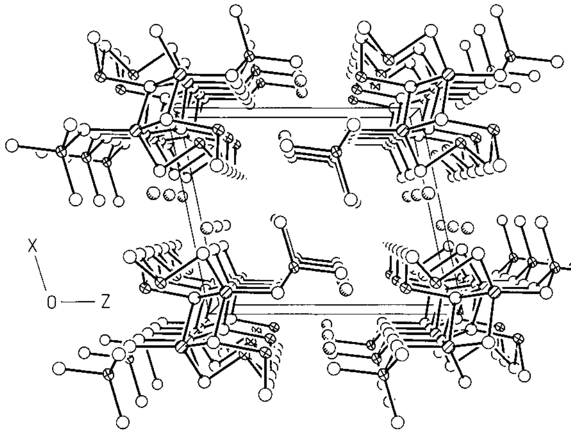

Figure 1. Unit-cell view, down the *b* axis, for $Cs_3Ag_2Sb_3S_8$ (**I**). Cesium atoms are highlighted, antimony atoms are boundary ellipsoids, silver atoms are shaded (left to right), and sulfur atoms are open spheres.

ing neighboring apical positions of the AgS_4 tetrahedra. The Sb−S bond lengths range from 2.308(9) to 2.339(6) Å with bond angles which only vary from 105.1(2) to 113.7(3)°, forming quite regular tetrahedra. These distances and angles are similar to those found in $K_3SbS_4 \cdot 4.5H_2O$[10] and $Na_3SbS_4 \cdot 9H_2O$,[11] which contain isolated SbS_4^{3-} tetrahedra. The $[SbS_2]_\infty^-$ chains are generated by vertex-shared SbS_3^{3-} pyramids which have their terminal sulfur atoms bridged to silver atoms. Bond distances for the pyramidal antimony atoms range from 2.385(7) to 2.497 (6) Å and bond angles vary from 91.8(3) to 98.6(2)° (Tables 3 and 4). The previously reported compounds $Cs_2Ag_3Sb_3S_7$[12] and $ASbS_2$ (A = Na,K,Cs)[13] also contain $[SbS_2]_\infty^-$ chains with similar bond distances and angles. There are very few chalcogenide compounds which contain mixed oxidation state antimony atoms. One example which contains Sb(III) and Sb(V) centers is $HgSb_4S_8$,[14] the synthetic form of the mineral livingstonite. Compound **I**, with tetrahedrally coordinated Sb(V) and pyramidally coordinated Sb(III) atoms, is the only phase synthesized in these laboratories which exhibits such mixed oxidation states of the pnictide metal.

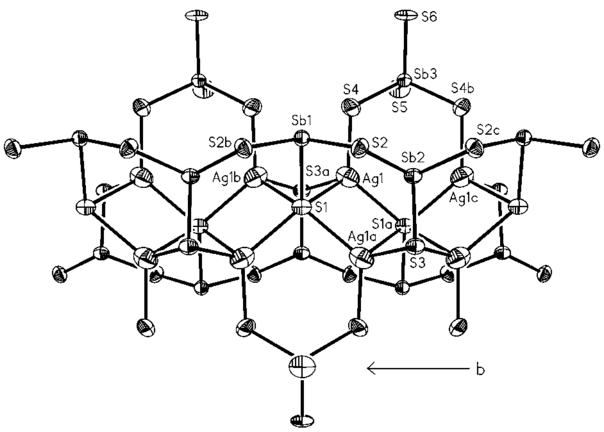

Figure 2. ORTEP representation (70% thermal ellipsoids) of a fragment of the infinite column found in $Cs_3Ag_2Sb_3S_8$ (**I**).

The linking silver atoms are all tetrahedrally coordinated to sulfur atoms from the $[SbS_2]_\infty^-$ chains and SbS_4^{3-} tetrahedra. These AgS_4 units are very distorted with bond distances ranging from 2.472(6) to 2.799(6) Å, and bond angles that vary from 98.5(2) to 126.9(2)°. Extreme distortions such as these are not uncommon in this type of system. For example, bond distances and angles range from 2.56 to 2.85 Å and 97 to 116°, respectively, in $Ba_2LaAg_5S_6$[15] and 2.49 to 2.89 Å and 95 to 139° in $CsAgSb_4S_7$.[12] In $Cs_3Ag_2Sb_3S_8$, the distortions observed are not the result of any silver−silver interactions but rather because of the rigidity of the antimony sulfide groups. Indeed, the SbS_4^{3-} groups hold the silver atoms apart, as evidenced by the Ag···Ag distances parallel to the *b* axis (3.23 Å for Ag1···Ag1a and 4.00 Å for Ag1···Ag1b). This is also a result of the silver atoms not residing on the mirror planes.

In **I**, the nearest S···S contacts from the terminal sulfur atoms on the SbS_4^{3-} groups to neighboring SbS_4^{3-} tetrahedra are greater that 3.8 Å. The nearest-neighbor contacts of the $[SbS_2]_\infty^-$ chains to sulfur atoms in other columns are greater than 3.2 Å, thus indicating the isolated nature of the anionic chains. The protruding SbS_4^{3-} tetrahedra, clearly evident in Figure 1, provide the necessary space for two types of cesium atom environments. One of the cesium cations, Cs1, has nine long contacts to sulfur atoms, which average 3.7(2) Å and are arranged in a distorted tricapped trigonal prismatic geometry. Cs2 is seven coordinate to sulfur, in a distorted hexagonal pyramid, with bond distances that average 3.71(6) Å. The remaining crystallographically unique cesium atom, Cs3, is located between adjacent columns and, like Cs1, has contacts to nine sulfur atoms that also average 3.7(1) Å and are arranged in a tricapped trigonal prismatic coordination envi-

---

(10) Mayer, H.; Mereiter, K. *Monatsh. Chem.* **1992**, *123*, 515.

(11) Mereiter, K.; Preisinger, A. *Acta Crystallogr.* **1979**, *B35*, 19.

(12) Jerome, J. E.; Schimek, G. L.; Pennington, W. T.; Kolis, J. W. Southeast/Southwest ACS Joint Regional Meeting, Nov 1995.

(13) (a) Lazarev, V. B.; Salov, A. V.; Berol, S. I. *Russ. J. Inorg. Chem.* **1979**, *24*, 313. (b) Graf, H. A.; Schäfer, H. *Z. Anorg. Allg. Chem.* **1975**, *414*, 211. (c) Kanishcheva, A. S.; Mikhailov, Y. N.; Kuznetsov, V. G.; Batog, V. N. *Dokl. Acad. Nauk. SSR* **1980**, *251*, 603.

(14) (a) Niizeki, N.; Buerger, M. J. *Z. Kristallogr.* **1957**, *109*, 129. (b) Srikrishnan, T.; Nowacki, W. *Z. Kristallogr.* **1975**, *141*, 174.

(15) Wu, P.; Ibers, J. A. *Z. Kristallogr.* **1993**, *208*, 35.

Table 3. Selected Bond Distances (Å)

$Cs_3Ag_2Sb_3S_8$ (**I**)			
Sb1−S1	2.472(8)	Cs1−S5	3.767(8)
Sb1−S2	2.497(6) ×2	Cs1−S5a	3.629(2) ×2
Sb2−S2	2.497(6) ×2	Cs1−S6	3.538(9)
Sb2−S3	2.385(7)	Cs2−S2	3.798(5) ×2
Sb3−S4	2.339(6) ×2	Cs2−S4	3.651(6) ×2
Sb3−S5	2.308(9)	Cs2−S6	3.700(9)
Sb3−S6	2.315(8)	Cs2−S6a	3.670(2) ×2
Ag1−S1	2.630(5)	Cs3−S1	3.463(8)
Ag1−S1a	2.799(6)	Cs3−S2	3.782(5) ×2
Ag1−S3a	2.648(7)	Cs3−S2a	3.507(6) ×2
Ag1−S4	2.472(6)	Cs3−S3	3.794(3) ×2
Cs1−S2	3.958(6) ×2	Cs3−S3a	3.635(8)
Cs1−S3	3.569(7)	Cs3−S5	3.614(9)
Cs1−S4	3.833(7) ×2		
α-Cs_2AgSbS_4 (**II**)			
Sb1−S1	2.349(4)	Cs1−S3	3.585(5)
Sb1−S2	2.341(5)	Cs1−S3a	3.869(5)
Sb1−S3	2.345(4)	Cs1−S4	3.740(5)
Sb1−S4	2.309(4)	Cs2−S1	3.477(5)
Ag1−S1	2.923(5)	Cs2−S2	3.739(5)
Ag1−S1a	2.604(5)	Cs2−S2a	3.591(5)
Ag1−S2	2.583(5)	Cs2−S3	3.887(5)
Ag1−S3b	2.480(4)	Cs2−S3a	3.413(5)
Cs1−S1	3.520(5)	Cs2−S4	3.662(6)
Cs1−S1a	3.585(5)	Cs2−S4a	3.743(5)
Cs1−S2	3.544(5)	Cs2−S4b	3.822(5)
Cs1−S2a	3.588(5)		
β-Cs_2AgSbS_4 (**III**)			
Sb1−S1	2.346(4)	Cs1−S4	3.634(5)
Sb1−S2	2.334(5)	Cs1−S4a	3.736(5)
Sb1−S3	2.346(4)	Cs1−S4b	3.714(4)
Sb1−S4	2.321(5)	Cs2−S1	3.634(4)
Ag1−S1	2.881(5)	Cs2−S1a	3.553(4)
Ag1−S1a	2.566(4)	Cs2−S2	3.799(5)
Ag1−S2	2.613(4)	Cs2−S2a	3.692(5)
Ag1−S3b	2.479(4)	Cs2−S2b	3.559(5)
Cs1−S1	3.548(5)	Cs2−S3	3.625(5)
Cs1−S2	3.657(4)	Cs2−S3a	3.922(5)
Cs1−S3	3.392(4)	Cs2−S4	4.025(4)
Cs1−S3a	3.573(4)		
Cs_2AgAsS_4 (**IV**)			
As1−S1	2.180(3)	Cs1−S4	3.588(4)
As1−S2	2.173(3)	Cs1−S4a	3.605(4)
As1−S3	2.179(3)	Cs1−S4b	3.669(3)
As1−S4	2.155(3)	Cs2−S1	3.682(3)
Ag1−S1	2.831(4)	Cs2−S1a	3.533(3)
Ag1−S1a	2.587(3)	Cs2−S2	3.879(4)
Ag1−S2	2.610(3)	Cs2−S2a	3.607(3)
Ag1−S3b	2.478(3)	Cs2−S2b	3.502(3)
Cs1−S1	3.512(4)	Cs2−S3	3.623(4)
Cs1−S2	3.644(3)	Cs2−S3a	3.821(3)
Cs1−S3	3.399(3)	Cs2−S4	3.804(3)
Cs1−S3a	3.622(3)		

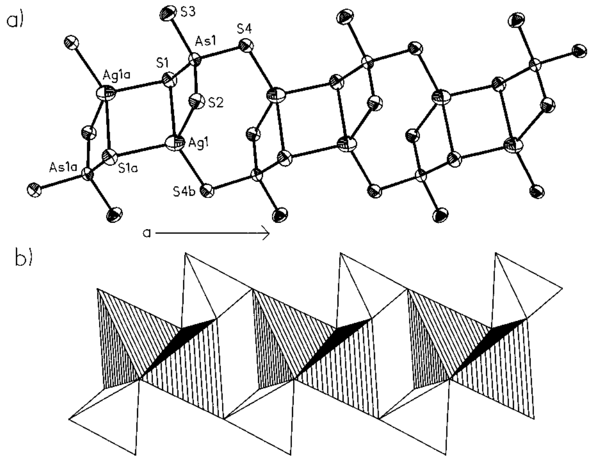

Figure 3. (a) ORTEP representation (70% thermal ellipsoids) of a fragment of the infinite column found in Cs_2AgAsS_4 (**IV**). (b) Polyhedral view of a $[AgMS_4]^{2-}$ column; silver tetrahedra are highlighted and pnictide tetrahedra are open.

Table 4. Selected Bond Angles (degrees)

$Cs_3Ag_2Sb_3S_8$ (**I**)			
S1−Sb1−S2	98.6(2) ×2	S1a−Ag1−S4	126.9(2)
S2−Sb1−S2b	93.8(3)	S3a−Ag1−S4	113.2(2)
S2−Sb2−S2c	91.8(3)	Sb1−S1−Ag1	89.2(2)
S2−Sb2−S3	96.6(2) ×2	Sb1−S1−Ag1a	126.1(2)
S4−Sb3−S4b	109.5(3)	Ag1−S1−Ag1a	77.9(1)
S4−Sb3−S5	111.5(2) ×2	Ag1−S1−Ag1b	70.6(2)
S5−Sb3−S6	113.7(3)	Ag1a−S1−Ag1b	132.1(3)
S4−Sb3−S6	105.1(2) ×2	Ag1a−S1−Ag1d	99.0(2)
S1−Ag1−S1a	102.1(1)	Sb1−S2−Sb2	99.9(2)
S1−Ag1−S4	100.4(2)	Sb2−S3−Ag1a	84.4(2)
S1−Ag1−S3a	98.5(2)	Ag1−S3a−Ag1b	75.3(2)
S1a−Ag1−S3a	110.1(2)	Sb3−S4−Ag1	110.1(2)
α-Cs_2AgSbS_4 (**II**)			
S1−Sb1−S2	106.3(2)	S1−Ag1−S3b	116.9(1)
S1−Sb1−S3	109.1(2)	S1a−Ag1−S3b	103.3(2)
S1−Sb1−S4	113.5(2)	S2−Ag1−S3b	128.4(2)
S2−Sb1−S3	109.6(2)	Sb1−S1−Ag1	79.4(1)
S2−Sb1−S4	110.0(2)	Sb1−S1−Ag1a	111.6(2)
S3−Sb1−S4	108.3(2)	Ag1−S1−Ag1a	68.6(1)
S1−Ag1−S1a	111.4(1)	Sb1−S2−Ag1	87.1(1)
S1−Ag1−S2	85.7(1)	Sb1−S3−Ag1b	112.3(2)
S1a−Ag1−S2	110.3(2)		
β-Cs_2AgSbS_4 (**III**)			
S1−Sb1−S2	107.3(1)	S1−Ag1−S3b	116.8(1)
S1−Sb1−S3	107.5(1)	S1a−Ag1−S3b	110.2(1)
S1−Sb1−S4	113.1(2)	S2−Ag1−S3b	124.1(2)
S2−Sb1−S3	110.2(2)	Sb1−S1−Ag1	79.7(1)
S2−Sb1−S4	108.9(1)	Sb1−S1−Ag1a	111.7(1)
S3−Sb1−S4	109.7(1)	Ag1−S1−Ag1a	74.9(1)
S1−Ag1−S1a	105.1(1)	Sb1−S2−Ag1	85.8(1)
S1−Ag1−S2	86.5(1)	Sb1−S3−Ag1b	111.7(1)
S1a−Ag1−S2	110.8(1)		
Cs_2AgAsS_4 (**IV**)			
S1−As1−S2	108.2(1)	S1−Ag1−S3b	123.1(1)
S1−As1−S3	107.7(1)	S1a−Ag1−S3b	112.4(1)
S1−As1−S4	112.3(1)	S2−Ag1−S3b	125.6(1)
S2−As1−S3	110.1(1)	As1−S1−Ag1	82.2(1)
S2−As1−S4	109.6(1)	As1−S1−Ag1a	113.4(1)
S3−As1−S4	108.9(1)	Ag1−S1−Ag1a	80.2(1)
S1−Ag1−S1a	99.8(1)	As1−S2−Ag1	87.7(1)
S1−Ag1−S2	80.7(1)	As1−S3−Ag1b	110.9(1)
S1a−Ag1−S2	109.4(1)		

ronment. These Cs−S bond distances are in keeping with those in similar compounds.[2d,2j,12,16]

The anionic chains, $AgMS_4^{2-}$, in **II**−**IV** contain identical connectivity. An isolated MS_4^{3-} tetrahedra and its inversion-generated partner are bridged together by Ag(I) ions, as shown in Figure 3. The infinite one-dimensional columns propagate parallel to the *a* axis (Figure 4). The MS_4^{3-} tetrahedra have nearly ideal geometry, with bond distances that vary from 2.31 to 2.35 Å when M = Sb and 2.16 to 2.18 Å when M = As; bond angles extend from 106 to 114° for **II**−**IV** (Tables 3 and 4). The coordination geometry and bond distances are typical for antimony[10,11] and arsenic.[17] As in $Cs_3Ag_2Sb_3S_8$, the Ag(I) ions are in a very distorted tetrahedral coordination environment. Two of the sulfur atoms coordinated to the silver are vertex-shared from two different M tetrahedra while the other two sulfurs are through edge-shared connections to the MS_4^{3-}. The Ag−S bond distances and angles range from 2.47 to 2.93 Å and 81 to 126°, respectively, with slight deviations among **II**−**IV**. The shortest silver−silver contact is 3.12 Å in the α phase; however the β phases are greater than 3.3 Å, thus implying that no metal−metal interactions are present in either form.

The main difference between the α and β forms is only due to packing considerations. Compound **II** has four formula units per unit cell, and **III** and **IV** have two formula units per unit cell, with approximately half the volume. The nearest

---

[16] Zhang X.; Kanatzidis, M. G. *Inorg. Chem.* **1994**, *33*, 1238.

[17] Pertlik, F. *J. Solid State Chem.* **1994**, *112*, 170 and references therein.

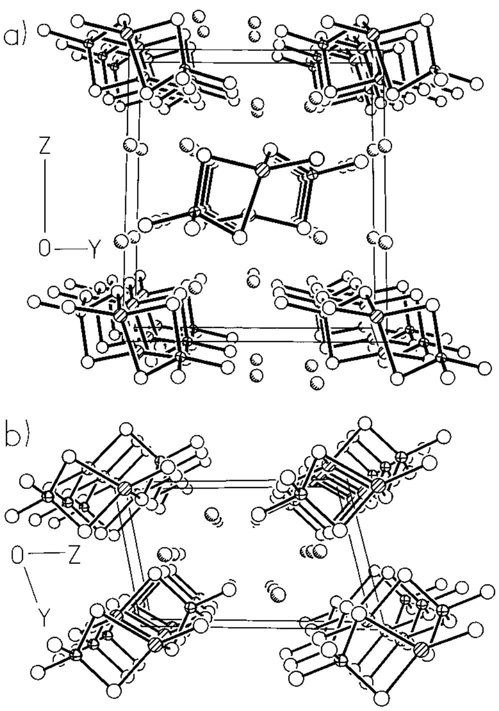

Figure 4. (a) Packing of the anionic columns, down the a axis, for α-Cs_2AgSbS_4 (**II**). (b) Packing of the anionic columns, down the a axis, for β-Cs_2AgSbS_4 (**III**). Cesium atoms are highlighted, antimony atoms are boundary ellipsoids, silver atoms are shaded (left to right), and sulfur atoms are open spheres.

interchain S$\cdots$S contacts are greater than 3.65 Å. These isolated $AgMS_4^{2-}$ columns are held apart by two crystallographically unique cesium atoms in **II**–**IV**, as shown in Figure 4. The coordination environment for Cs1 is a distorted, monocapped octahedron with Cs–S bond lengths that range from approximately 3.39 to 3.87 Å. Similarly, Cs2 is eight coordinate to sulfur, in a distorted bicapped octahedral geometry, with Cs–S bond lengths that range from 3.47 to 4.03 Å. These Cs–S bond distance are similar to phases already mentioned.

Discussion

Compounds **I** and **IV** appear to be indefinitely stable toward air and moisture after the removal of the mother liquor; however, both forms of Cs_2AgSbS_4 are quite moisture sensitive. The α and β forms of Cs_2AgSbS_4 cannot be prepared separately. A few observations about the Cs_2AgMS_4 (M = Sb or As) systems favor the β triclinic form as the more thermodynamically stable phase. From a sampling of approximately 10 crystals in the Cs_2AgMS_4 systems in which reaction conditions were varied, the lattice parameters for the α form were obtained only once from single-crystal indexing. The structural refinements of **II** and **III** are comparable and were both collected at room temperature. The average thermal motion of **II** is larger than that of **III**, implying that it has greater entropy. And finally, **II** has a slightly lower density than **III**, suggesting that the packing in the monoclinic α form is less efficient. Thus the triclinic β forms of Cs_2AgMS_4 appear to be slightly more stable than the α form.

Bond strengths of the metal–sulfur bonds were calculated from the empirical relationship developed by Brown and Altermatt.[18] The sum of all the individual metal–sulfur bond strengths about a given metal atom results in the valence of that atom. The premise for this type of calculation is to be able to decide the valence of atoms based strictly upon bond distances, given a predetermined distance for a specific metal–sulfur single bond. All calculated valences are summarized in Table 5 and agree with the expected oxidation states of the metal centers. For example, the calculated valence states for the unique antimony atoms in **I** (2.88, 3.15, and 5.14) clearly illustrate the different formal oxidation states. The cumulative result from these bond valence sums is that all four phases are electron precise, assuming S^{2-} is present in all cases. The coordination about the pnictides of these four compounds also predicts their oxidation states because the lone pairs are stereochemically active. Thus the three-coordinate Sb(III) centers are in pyramidal coordination environments in $[SbS_2]_\infty^-$, while the four-coordinate group 15 M(V) centers are tetrahedral.

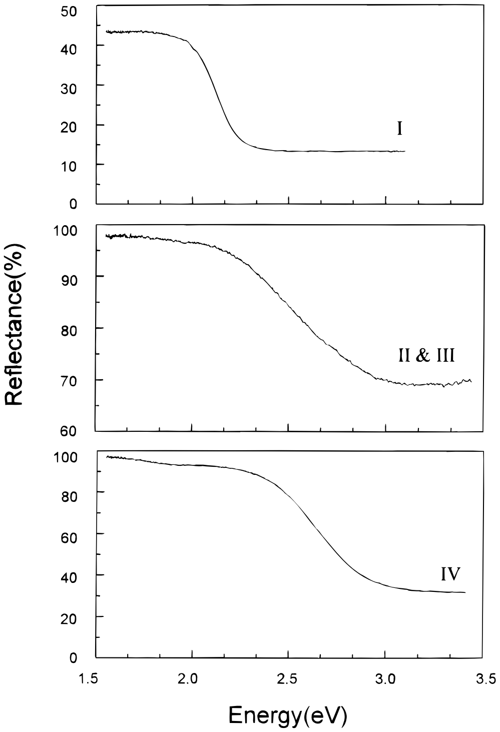

Figure 5. Diffuse reflectance spectra of compounds **I**–**IV**.

Table 5. Bond Valence Sums for I–IV

	I	II	III	IV
antimony	2.88(5) 3.15(5) 5.14(10)	4.98(5)	4.98(6)	4.94(4)
silver	1.04(2)	1.05(1)	1.07(1)	1.07(1)
cesium	1.07(1) 0.87(1) 1.19(1)	1.09(1) 1.19(1)	1.17(1) 1.01(1)	1.25(1) 1.11(1)

Optical diffuse reflectance measurements on **I**, **II** and **III** (indistinguishable polymorphs), and **IV** confirmed that these materials are electronically precise and are either wide-bandgap semiconductors or poor insulators. $Cs_3Ag_2Sb_3S_8$ (**I**) and Cs_2AgAsS_4 (**IV**) exhibit linear absorption[2] versus energy curves near their respective absorption edges. This relationship is characteristic of materials with direct bandgaps.[19] Therefore the bandgap is derived by extrapolating the linear portion of the

---

(18) Brown, I. D.; Altermatt, D. *Acta Crystallogr.* **1985**, *B41*, 244.

(19) Pankove, J. I. *Optical Processes in Semiconductors*; Prentice Hall, Inc.: New Jersey, 1971.

absorption edge to $(\alpha/s)^2 = 0$, where $h\nu \cong E_g$. Both forms of Cs_2AgSbS_4, which were not separable, show a relatively linear fit for absorption^2 (direct) or absorption$^{1/2}$ (indirect) versus energy. Thus, the nature of the bandgap is not clear. This behavior may be the result of the broad transition due to the mixed membered (**II** and **III**) phases. The average bandgap, E_g, was determined by the inflection point in the first-derivative curve of reflectance versus energy for Cs_2AgSbS_4. Figure 5 shows the spectra from which bandgaps of 2.1, 2.5, and 2.7eV were derived for **I**, **II**/**III**, and **IV**. Attempts to determine the electrical conductivity of these compounds using the four-probe technique were not reliable because of their high room-temperature resistivity, generally between 10^6 and 10^8 Ω cm. However, a four-probe measurement[20] of a single crystal of **I** from 298 to 200 K was attempted and showed increasing resistivity with decreasing temperature, also supporting the postulate that these compounds are poor semiconductors.

The compounds described here can be viewed as either metalated derivatives of Zintl phases[21] or relatives of sulfo salts.[22] Sulfo salts, as defined by mineralogists, are structurally complex solids formed by MS_3^{3-} groups bridged to a variety of soft metal centers. Thus **I** can be considered a sulfo salt derivative or anionic (reduced) sulfo salt, in which silver acts as the metal center. None of the individual coordination environments observed in **I**−**IV** are unique; however, the structures are all novel and indicate that the use of supercritical ammonia is a viable route to an enormous variety of new compounds.

Acknowledgment. We are indebted to the National Science Foundation and Petroleum Research Foundation for support of this work. We are grateful to Bill Pennington for helpful discussions regarding the crystallography and Shiou-Jyh Hwu and Richard A. Mackay for assistance with the conductivity apparatus and interpretation of the data.

Supporting Information Available: Complete crystallographic information, anisotropic thermal parameters, and bond angles for **I**−**IV**, as well as plots of energy vs absorption^2 and absorption$^{1/2}$ (21 pages); list of observed and calculated structure factors (19 pages). Ordering information is given on any current masthead page.

CM950392M

---

[20] van der Pauw, L. J. *Phillips Res. Rep.* **1958**, *13,* 1.

[21] Schäfer, H. *Annu. Rev. Mater. Sci.* **1985**, *15,* 1.

[22] (a) Berry, L. G.; Mason, B. In *Minerology*; W. H. Freeman: San Francisco, **1959**. (b) Takeuchi, Y.; Sadanaga, R. *Z. Kristallogr.* **1969**, *130,* 346. (c) Hellner, E. *J. Geol.* **1958**, *66,* 503.